THE JOURNAL OF PHYSICAL CHEMISTRY C

Article

Cite This: J. Phys. Chem. C 2018, 122, 21667−21676

pubs.acs.org/JPCC

Systematic Comparison of Carbon Dots from Different Preparations—Consistent Optical Properties and Photoinduced Redox Characteristics in Visible Spectrum and Structural and Mechanistic Implications

Lin Ge,[†] Nengyu Pan,[†] Jirui Jin,[†] Ping Wang,*[,†] Gregory E. LeCroy,[†] Weixiong Liang,[†] Liju Yang,*[,‡] Lindsay R. Teisl,[†] Yongan Tang,[§] and Ya-Ping Sun*[,†]

[†]Department of Chemistry and Laboratory for Emerging Materials and Technology, Clemson University, Clemson, South Carolina 29634, United States

[‡]Department of Pharmaceutical Sciences, Biomanufacturing Research Institute and Technology Enterprise, and [§]Department of Mathematics and Physics, North Carolina Central University, Durham, North Carolina 27707, United States

ABSTRACT: Carbon dots (CDots) are characterized by their optical properties including strong absorptions and bright and colorful fluorescence emissions in the visible spectrum and by their photoinduced redox characteristics as both potent electron acceptors and donors. The reported study was for a systematic comparison of CDots from different synthetic approaches based on the use of pre-existing small carbon nanoparticles sourced from pure carbon soot versus the formation of similar nanoparticles in situ via a one-pot thermal carbonization of organic molecular precursors, emphasizing spectroscopic characterizations over the visible spectrum. The results show that the CDots prepared by the latter under sufficiently robust processing conditions are generally no different from those from the former in terms of the observed optical properties and associated photoinduced redox characteristics in the application-wise more meaningful visible spectral region, suggesting a high stability or general applicability of the definition on CDots as surface-passivated small-carbon nanoparticles. Implications of the reported findings to the further understanding and mechanistic explorations of CDots, including the necessity to focus on the core carbon nanoparticles in CDots in such explorations, are highlighted and discussed.

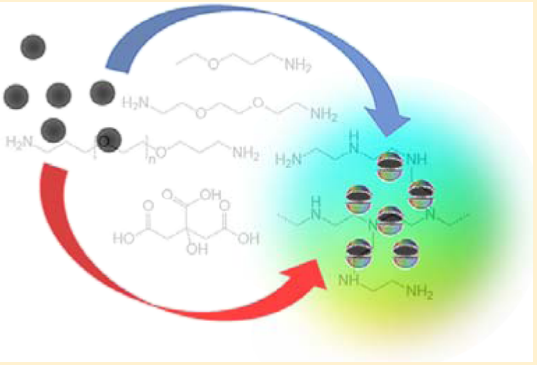

INTRODUCTION

Carbon "quantum" dots or carbon dots (CDots) are generally defined as small carbon nanoparticles with various surface-passivation schemes (Figure 1).[1−3] Ever since their original finding,[1] there have been broad and intense interests in CDots for their unique and/or advantageous properties.[4] A wide variety of potential technological applications of CDots have been pursued, including bioimaging and sensing,[5−10] photocatalytic energy conversions and optoelectronics,[11−16] antibacterial and antiviral functions,[17−21] and others.[22−28] In fact, CDots now represent a rapidly advancing and expanding research field, as reflected by the large and ever increasing number of publications in the recent literature.[4,29−41]

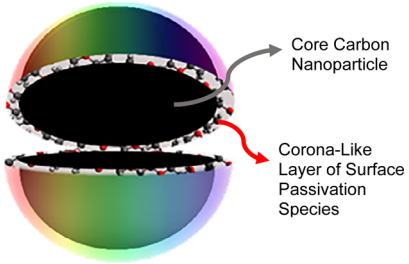

Figure 1. Cartoon illustration on CDot, which is generally a small carbon nanoparticle core with attached surface passivation molecules in a configuration similar to a soft corona-like shell.

CDots are known for their characteristic optical properties, with their observed optical absorptions because of electronic transitions in the underlying carbon nanoparticles and their generally bright and excitation wavelength-dependent fluorescence emissions.[1,33] Among the various syntheses of CDots, the deliberate chemical functionalization method developed in the original finding of CDots is such that specifically processed and selected small carbon nanoparticles are chemically functionalized by oligomeric and polymeric molecules for the surface passivation purpose,[1,42,43] thus more closely adhering to the general definition on CDots (Figure 1). The method has also been credited for the preparation of some of the best-

Received: July 24, 2018
Revised: August 29, 2018
Published: August 30, 2018

DOI: 10.1021/acs.jpcc.8b06998
J. Phys. Chem. C 2018, 122, 21667−21676

performing CDots with respect to bright and colorful fluorescence emissions.[42,44] However, most of the reported syntheses of CDots in the literature have been based on the carbonization of organic molecules or other carbon-containing precursors, often in "one-pot" processing with or without the involvement of a solvent.[4,29−41] A rationale for the carbonization method in relationship to the general definition on CDots (Figure 1) may be such that the carbonization of organic precursors for the formation of core carbon nanoparticles is incomplete, and thus the remaining organic species attached to or associated with the carbon nanoparticles formed as a result of the carbonization would serve the required surface passivation function. For example, citric acid (CA)−oligomeric polyethylenimine (PEI) mixtures have been used as precursors in the thermal carbonization processing under various conditions for the synthesis of CDots.[45−48] A more popular processing condition for such a synthesis has been the hydrothermal (HT) treatment of a CA−PEI mixture at a temperature up to 200 °C for a few hours, yielding materials with absorption and fluorescence emissions mostly in the UV region, significantly different from those of the CDots from the deliberate chemical functionalization synthesis.[43] More recently, it was shown that the popular HT processing condition was inadequate or insufficient for the carbonization purpose,[49−52] and that with more robust conditions including the use of significantly higher processing temperatures, a much better agreement could be achieved between the CDots thus prepared and those from the deliberate chemical functionalization method in terms of their observed optical and other properties.[49] This example is representative, pointing to a broad need for systematic comparisons of CDots from different syntheses and/or under various synthesis conditions, in reference to the general definition on CDots (Figure 1), because there have been so many reported studies of CDots based on samples prepared from the carbonization processing of organic precursors under likely overly mild conditions. In fact, there have been increasing concerns and confusions in the literature[50−55] on the samples from carbonization syntheses under mild processing conditions, such as those in the HT reaction referred to the above.[45−47,56−59] These samples generally exhibit absorptions predominantly in the UV spectral region, often corresponding to mostly excitation-wavelength-independent fluorescence emissions. The spectroscopic results have promoted debates on the actual content and role of nanoscale carbon (the foundation for CDots conceptually and structurally) in these samples, with suggestions such that the observed optical properties could be because of various collections of different chromophores produced in the carbonization processing.[51−55] Because the UV spectral region, especially the region shorter than 350 nm, is intrinsically messy spectroscopically because of potential absorptions or strong absorptions of many functional groups associated with the altered, derivatized, and/or reacted organic species in the precursor mixture used in the carbonization processing, a resolution of the ongoing debates or controversies toward a clear and unified understanding of the carbonization synthesis and the CDots platform in general is understandably more challenging. For the visible spectral region, on the other hand, the dominance of carbon nanoparticles in optical absorptions would make the comparison of CDots from different preparations much less complicated. The results thus obtained should be highly valuable to the unified understanding discussed above and ultimately to address the issues in the UV spectral region.

In the study reported here, optical properties in the visible spectrum and associated photoinduced redox characteristics were investigated systematically for the dot samples obtained from different syntheses and under various experimental conditions. The CDots from the deliberate chemical functionalization method were used as reference for the fact that the core carbon nanoparticles in these CDots are pre-existing, dominating optical absorptions in the visible spectrum and the subsequent photoexcited state properties and processes. In addition to the comparison between these CDots and those from the thermal carbonization syntheses with organic precursors, CDots prepared by a hybrid method that combines the use of pre-existing carbon nanoparticles and their functionalization by organic species under thermal reaction conditions were also included for the comparison. Results from the comparisons show a general agreement among the different dot samples for their optical properties over the visible spectral region, suggesting the general applicability and high stability of the definition on CDots. Here, the "general agreement" referred to the above requires more vigorous conditions in the thermal carbonization synthesis of CDots, namely that when the carbonization processing is performed correctly under right conditions, the resulting CDots exhibit properties in the visible spectrum consistent with those of CDots from other syntheses. The emphasis in this study on the consistent optical properties and associated redox characteristics in the visible spectrum is aimed for the conclusion that at least in this spectral region (more relevant to most of the widely pursued applications of CDots anyway), the various CDots from different syntheses are consistent. As related, the significance and broader implications of the results to further validation of the general definition on CDots and mechanistic explorations are discussed.

EXPERIMENTAL SECTION

Materials. The carbon nanopowder sample (US1074) was acquired from US Research Nanomaterials, Inc. 2,2′-(Ethylenedioxy)bis(ethylamine) (EDA), 3-ethoxypropylamine (EPA), diamine-terminated oligomeric poly(ethylene glycol) (average molecular weight 1,500, PEG_{1500N}), *N*,*N*-diethylaniline (DEA), and 2,4-dinitrotoluene (DNT) were purchased from Sigma-Aldrich; CA and thionyl chloride from Alfa Aesar; oligomeric PEI (average molecular weight 600, branched) from Polysciences; and nitric acid from VWR. Dialysis membrane tubing (molecular weight cutoff 500 or 1000) was supplied by Spectrum Laboratories. Water was deionized and purified by being passed through a Labconco WaterPros water purification system.

Measurement. UV/vis absorption spectra (ABS) were recorded on Shimadzu UV2501 and UV-3600 spectrophotometers. Fluorescence spectra were acquired on a Jobin-Yvon emission spectrometer equipped with a 450 W xenon source, Gemini-180 excitation and Triax-550 emission monochromators, and a photon counting detector (Hamamatsu R928P PMT at 950 V). 9,10-Bis(phenylethynyl)-anthracene in cyclohexane was used as a standard in the determination of fluorescence quantum yields by the relative method (matching the absorbance at the excitation wavelength between the sample and standard solutions and comparing their corresponding integrated total fluorescence intensities). Fourier transform infrared spectroscopy (FT-IR) spectra were

DOI: 10.1021/acs.jpcc.8b06998
J. Phys. Chem. C 2018, 122, 21667−21676

measured on a Shimadzu IRAffinity-1S spectrometer with the single-reflection attenuated total reflection accessory for solid samples. Transmission electron microscopy (TEM) imaging was performed on a Hitachi H-9500 high-resolution TEM system.

Carbon Dots. The deliberate chemical functionalization method was used for the synthesis of CDots with EDA, 3-EPA, and the oligomeric polyethylene glycol diamine (molecular weight 1500, PEG_{1500N}) for surface functionalization–passivation, thus EDA-CDots,[43] EPA-CDots,[60] and PEG_{1500N}-CDots,[42,44,61] respectively (Figure 2). The small carbon

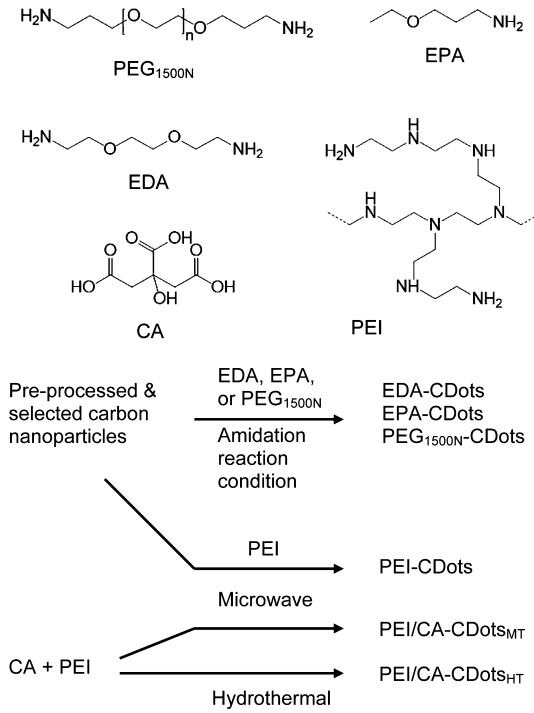

Figure 2. Molecules used for surface functionalization and/or as precursors for the various CDots, and the different reaction schemes for syntheses of the CDots under different processing conditions.

nanoparticles for the functionalization reactions were harvested from commercially acquired carbon nanopowders involving oxidative acid treatments. In a typical experiment, the carbon nanopowder sample (2 g) was refluxed in concentrated nitric acid (8 M, 200 mL) for 48 h. The reaction mixture was cooled back to ambient temperature and centrifuged at 1000*g* to discard the supernatant. The residue was redispersed in deionized water, dialyzed in a membrane tubing (molecular weight cutoff 500) against fresh water for 48 h, and then centrifuged at 1000*g* to retain the supernatant as an aqueous dispersion of small carbon nanoparticles. The nanoparticles could be recovered from the dispersion by removing water via evaporation.

For the synthesis of EDA-CDots as an example, the carbon nanoparticles (50 mg) were refluxed in neat thionyl chloride for 12 h. Upon the removal of excess thionyl chloride via evaporation, the treated carbon nanoparticles were carefully mixed with EDA (600 mg), heated to 120 °C, and stirred vigorously under nitrogen protection for 72 h. The reaction mixture was cooled to room temperature and dispersed in water and then centrifuged at 20 000*g* to retain the supernatant. The aqueous solution thus obtained was dialyzed against fresh water (molecular weight cutoff 500) to remove unreacted EDA and other small molecular species to yield the EDA-CDots as an aqueous solution. The EPA-CDots and PEG_{1500N}-CDots were similarly synthesized.

The CDots with oligomeric PEI (average molecular weight 600, branched) for surface functionalization–passivation, thus PEI-CDots (Figure 2), were prepared from the small carbon nanoparticles discussed above by thermally induced functionalization with PEI. In a typical experiment, the carbon nanoparticles (100 mg) as an aqueous slurry were mixed with PEI (2 g) and ethanol (2 mL) in a scintillation vial, and the resulting mixture was sonicated in an ultrasonic cleaner (VWR 250D) at 40 °C for 1 h, followed by a complete removal of solvent via evaporation for a solid mixture. Separately, a bath of silicon carbide (150 g) in a silica crucible casting dish (about 8 cm in diameter and 2.5 cm in height) was prepared and preheated in a conventional microwave oven at 500 W for 3 min. Several rounds of microwave treatments were as follows: (1) the vial containing the solid mixture was immersed in the preheated silicon carbide bath for microwave irradiation at 1000 W for 3 min; (2) the sample vial was taken out of the bath for being cooled in the ambient, and more PEI (1 g) and ethanol (2 mL) were added and mixed well, followed by the removal of ethanol, and then microwave irradiation of the same as in (1); (3) a repeat of (2) but with the microwave irradiation at 500 W for 8 min; and (4) a repeat of (3). After microwave treatments, the reaction mixture was cooled to ambient temperature and dispersed in deionized water with vigorous sonication. The resulting aqueous dispersion was centrifuged at 5000*g* to collect the supernatant, followed by dialysis (molecular weight cut-off 1000) against fresh water for 6 h to obtain the PEI-CDots in an aqueous solution.

The thermal carbonization of binary mixtures of the PEI and CA as precursors, with the carbonization via HT processing and microwave-assisted thermal (MT) processing, was used for the preparation of the PEI/CA-$CDots_{HT}$ and PEI/CA-$CDots_{MT}$, respectively (Figure 2). For the former, CA (3 g) was dissolved in water (6 mL) with mild sonication in an ultrasonic cleaner (VWR 250D). To the solution was added PEI (1.5 g) with stirring for a good mixing. The resulting aqueous mixture was loaded into a stainless steel tube reactor (1.9 cm OD × 30.5 cm length). The reactor was sealed and then heated in a tube furnace at 330 °C for 6 h. Post-processing, the reactor was cooled to ambient temperature, and the reaction mixture in the reactor was collected by washing with water (10 mL). The brownish aqueous solution thus obtained was centrifuged at 10 000*g* to retain the supernatant, followed by dialysis (molecular weight cut-off 1000) against fresh water to obtain the PEI/CA-$CDots_{HT}$.

For the PEI/CA-$CDots_{MT}$, CA (1 g) in water (2 mL) and PEI (3 g) were mixed well, and then water was removed via evaporation. The resulting solid mixture in a scintillation vial was immersed in the preheated silicon carbide bath described above for treatments with microwave irradiation, first at 200 W for about 4 min (no more bubbles in the sample, with the sample color turning dark orange) and then 1000 W for 3 min, during which there were five brief pauses each of a few seconds. Post-treatment, the reaction mixture was cooled to the ambient temperature and dispersed in deionized water with sonication. The resulting aqueous dispersion was centrifuged at 5000*g* to keep the supernatant, followed by dialysis (molecular weight cutoff 1000) against fresh water for 6 h to obtain the PEI/CA-$CDots_{MT}$ as a colored aqueous solution.

DOI: 10.1021/acs.jpcc.8b06998
J. Phys. Chem. C 2018, 122, 21667–21676

For microscopy analyses, some of the dot samples described above were doped with a small amount of silver via simple visible-light photolysis in an aqueous solution of a silver salt.[62] The doping level was kept very low, as monitored in terms of the very onset in the initial emergence of the silver plasmon absorption band.

RESULTS AND DISCUSSION

For comparisons, CDots with selected small or oligomeric amino molecules for surface passivation (Figure 2) were prepared by using the three major synthetic approaches:[4,29−41] (1) the deliberate chemical functionalization of pre-processed and selected small carbon nanoparticles,[42−44,60] (2) the carbonization of binary organic mixtures as precursors in HT and MT processing,[49] and (3) the method of essentially a hybrid of the other two in which the small carbon nanoparticles are functionalized by the selected amino molecules under carbonization-like thermal-processing conditions.[63] A distinctive attribute of the first approach is with the use of pre-existing carbon nanoparticles for surface chemical functionalization under rather mild amidation reaction conditions, which are impossible to derivatize the simple aliphatic amino molecules (EDA, EPA, and PEG_{1500N}, in this work) into any organic dyes of significant optical absorptions in the visible spectral region. Thus, the only species in the sample solutions responsible for the observed absorptions and fluorescence emissions in the visible spectral region have to be the surface-passivated carbon nanoparticles. The CDots thus prepared are ideally suited for the reference role in comparison with those from other syntheses. Specifically for the EDA-CDots,[43] EPA-CDots,[60] and PEG_{1500N}-CDots,[42,44,61] Figure 2, their visible absorption and fluorescence spectra in aqueous solutions are shown in Figure 3, and the corresponding fluorescence quantum yields and lifetimes are summarized in Table 1. The absorption spectrum of the EDA-CDots tracks well that of the aqueous-dispersed small carbon nanoparticles used as a precursor in the dot syntheses, reaffirming the conclusion that optical absorptions by CDots over the visible spectrum are dictated by the core carbon nanoparticles because EDA molecules for the surface functionalization are completely transparent across the near-UV to visible spectral regions. The spectrum of the PEG_{1500N}-CDots is similar, except for some extra absorptions in the blue spectral region beyond those of the carbon nanoparticles (Figure 3). When excited into the specific portion of the absorption spectrum with extra absorptions (around 440 nm), the fluorescence emissions were significantly brighter, but without any significant changes in the emission spectral profile (Figure 3). These absorption and fluorescence spectral features have been attributed to special surface passivation effects associated with the functionalization of small carbon nanoparticles by a selected group of surface passivation agents including PEG_{1500N}.[42,60] Such effects are particularly pronounced in the EPA-CDots, with more pronounced extra absorptions (Figure 3) and the corresponding fluorescence emissions of higher quantum yields (Table 1). Despite these additional spectroscopic features, however, the CDots from the deliberate chemical functionalization synthesis are structurally simple and consistent, serving as the foundation for the general definition on CDots.

The carbonization of organic precursors has been more popular in the literature for the preparation of CDots or products/materials that are believed to be CDots-like, despite the fact that little effort has been made to compare

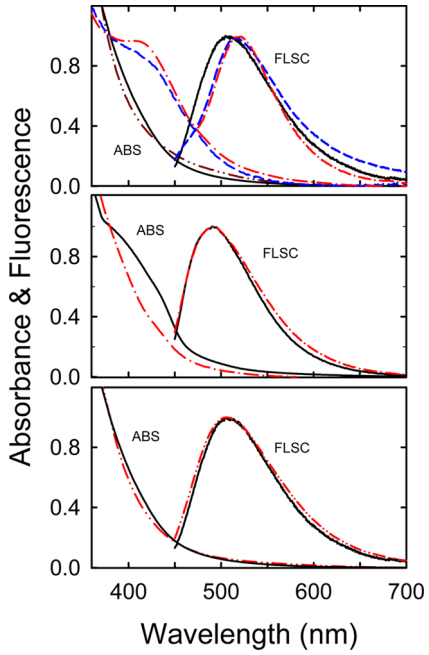

Figure 3. Absorption (ABS) and fluorescence (FLSC, 440 nm excitation) spectra in aqueous solution for (upper) EDA-CDots ( ), EPA-CDots (-.-.-), PEG_{1500N}-CDots (- - -), and for comparison (ABS only), the aqueous dispersed carbon nanoparticles (-..-..-); (middle) PEI/CA-$CDots_{HT}$ ( ) and PEI/CA-$CDots_{MT}$ (-.-.-); and (lower) PEI-CDots (-.-.-) and for comparison the EDA-CDots ( ).

Table 1. Fluorescence Quantum Yields and Lifetimes of the Various CDots

	fluorescence quantum yield		$\langle\tau_F\rangle$ (ns)[a]	
dot sample	λ_{EXC} 400 nm	λ_{EXC} 440 nm	λ_{EXC} 400 nm	λ_{EXC} 440 nm
EDA-CDots	0.24	0.14	7.2	7.2
EPA-CDots	0.31	0.35	6.1	8.3
PEG_{1500N}-CDots		0.25	6[b]	
PEI/CA-$CDots_{HT}$	0.5	0.45	14	14
PEI/CA-$CDots_{MT}$	0.25	0.18	12.5	12.5
PEI-CDots	0.28	0.14	8.1	7.4

[a]Average fluorescence lifetime from fitting each fluorescence decay with a biexponential function, $\langle\tau_F\rangle = (A_1\tau_{F1}^2 + A_2\tau_{F2}^2)/(A_1\tau_{F1} + A_2\tau_{F2})$. [b]407 nm excitation.

quantitatively optical absorptions of the presumed carbon nanoparticles formed in the carbonization with those of the solid carbon nanoparticles, such as those harvested from pure carbon soot, as discussed above. A potential danger with a lack of such a required rigorous comparison is that many of the carbonization products (especially those processed under rather mild experimental conditions) may have little to do with "CDots" other than the observation of fluorescence emissions associated with excitations mostly in the UV region. Again, the shorter wavelength UV region (<350 nm) is usually considered messy spectroscopically because of the fact that a large number of molecules and species containing aromatic (or the like) moieties or heteroatom-derived molecular structures can become luminescent impurities. Thus, in this study for the comparison of CDots from the carbonization processing, PEI/CA-$CDots_{HT}$ and PEI/CA-$CDots_{MT}$ (Figure 2) specifically,

DOI: 10.1021/acs.jpcc.8b06998
J. Phys. Chem. C 2018, 122, 21667−21676

with those from the deliberate chemical functionalization method as a reference, the focus was on the absorption and fluorescence emission properties in the visible spectrum where the photon harvesting is dictated by the carbon nanoparticles.

The preparation of the PEI/CA-CDots$_{HT}$ was similar to that reported previously.[49] For the PEI/CA-CDots$_{MT}$, a PEI−CA mixture without solvent was processed in microwave-assisted carbonization processing. Experimentally, the precursor mixture in a scintillation vial immersed in a silicon carbide bath was processed in a conventional microwave oven. Post-processing, the reaction mixture was dispersed in water, followed by centrifugation to keep the supernatant, which was then dialyzed against fresh water to obtain the desired dot sample as a colored aqueous solution.

The absorption and fluorescence spectra of the PEI/CA-CDots$_{HT}$ and PEI/CA-CDots$_{MT}$ are compared in Figure 3, also with those of the CDots discussed above, and other fluorescence parameters are provided in Table 1. In the comparison, ABS of the PEI/CA-CDots$_{HT}$ and PEI/CA-CDots$_{MT}$ are somewhat different with respect to the extra absorptions around 420−440 nm, which are more pronounced in the former (Figure 3). Correspondingly, fluorescence quantum yields of the PEI/CA-CDots$_{HT}$ are significantly higher (Table 1), yet fluorescence spectral profiles of the two samples are essentially the same (Figure 3). In terms of the same rationale discussed above on special passivation effects being responsible for the extra absorptions and the associated brighter fluorescence emissions, the results from the comparison suggest likely somewhat different surface structures of the dots in the two samples prepared from the same PEI−CA mixture as a precursor but under different carbonization processing conditions. The microwave-assisted processing was apparently less favorable to the kind of configuration in the surface passivation layer of the dots (Figure 1) responsible for the extra absorptions. The overall dot profiles as probed by TEM imaging are similar between the PEI/CA-CDots$_{HT}$ and PEI/CA-CDots$_{MT}$ (Figure 4). The lack of lattice fringes in the TEM images is consistent with the X-ray powder diffraction results suggesting mostly amorphous carbon in the dot structure, similar to the result for the preprocessed and selected small carbon nanoparticles (Figure 5). All of these diffraction patterns are very broad (Figure 5), without the peaks commonly associated with graphitic carbon, thus indicative of the lack of any defined crystalline structures in these carbon nanoparticles.

FT-IR spectra of the PEI/CA-CDots$_{HT}$ and PEI/CA-CDots$_{MT}$ are also rather similar, and both are different from those of the PEI and CA precursors (Figure 6). In the precursor mixture, the carboxylic acids in CA and amino groups in PEI likely formed zwitterionic pairs, some of which could have survived the carbonization processing conditions to be responsible for the absorptions in the carbonyl region (1770−1650 cm^{-1}, Figure 6). In both dot samples, the characteristic N−H and C−H absorptions are weaker and broader than those in the spectra of the precursor molecules, consistent with the consumption of those molecules in the carbonization processing and the generally more diverse local environments for the corresponding vibration modes.

In addition to the deliberate chemical functionalization method and the one-pot carbonization synthesis discussed above, CDots could also be prepared in a hybrid approach that combines some of the major features of the other two methods, including the use of preprocessed and selected small carbon nanoparticles for surface functionalization with organic species in thermal reactions to achieve the required or desired passivation effect. Because of the templating role provided by the carbon nanoparticles in the thermal processing, the resulting CDots should share a similar structural configuration with that of the dots from the deliberate chemical functionalization method, thus adhering equally closely to the general definition on CDots (Figure 1). Specifically for the PEI-CDots (Figure 2) in this work, the same preprocessed and selected small carbon nanoparticles discussed above were functionalized by the oligomeric PEI (average molecular

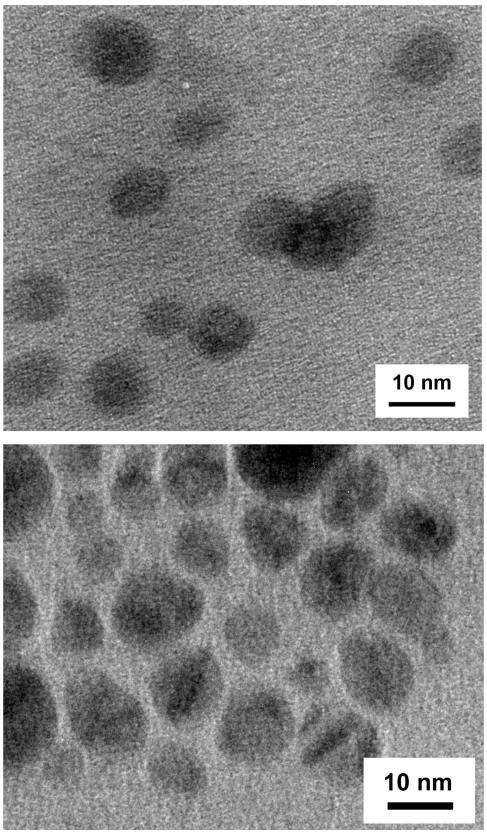

Figure 4. Representative TEM images of the PEI/CA-CDots$_{HT}$ (upper) and PEI/CA-CDots$_{MT}$ (lower) dispersed on silicon dioxide grids.

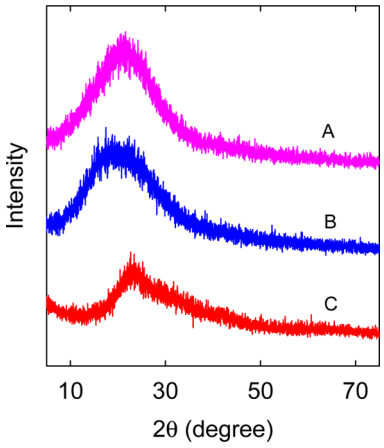

Figure 5. X-ray powder diffraction patterns of the (A) PEI/CA-CDots$_{MT}$, (B) PEI/CA-CDots$_{HT}$, and (C) preprocessed and selected small carbon nanoparticles.

DOI: 10.1021/acs.jpcc.8b06998
J. Phys. Chem. C 2018, 122, 21667−21676

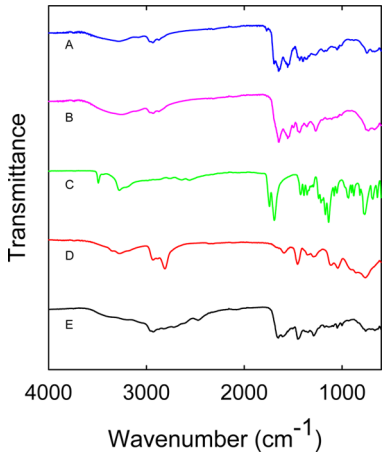

Figure 6. FT-IR spectra of (A) PEI/CA-CDots$_{HT}$, (B) PEI/CA-CDots$_{MT}$, (C) neat CA, (D) oligomeric PEI, and (E) PEI-CDots.

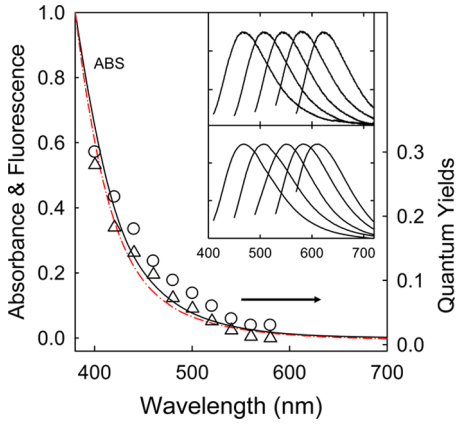

Figure 7. ABS and fluorescence quantum yields at different excitation wavelengths for the EDA-CDots (, ○) and PEI-CDots (-.-.-, Δ). Inset: Normalized fluorescence spectra of the EDA-CDots (upper) and PEI-CDots (lower) corresponding to excitations (from left to right) at 400, 440, 480, 520, and 560 nm.

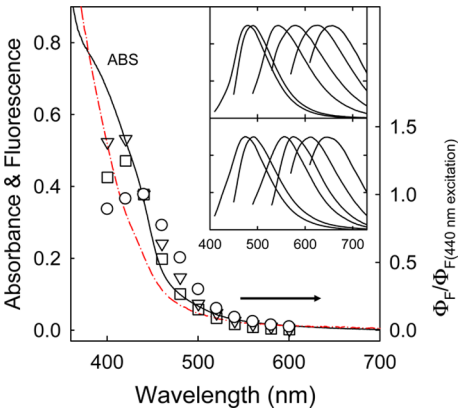

Figure 8. ABS and fluorescence quantum yields at different excitation wavelengths (normalized by dividing the value at 440 nm excitation, Table 1) for the PEI/CA-CDots$_{HT}$ (, ○) and PEI/CA-CDots$_{MT}$ (-.-.-, □) and for comparison, the EPA-CDots (quantum yields only, ▽). Inset: Normalized fluorescence spectra of the PEI/CA-CDots$_{HT}$ (upper) and PEI/CA-CDots$_{MT}$ (lower) corresponding to excitations (from left to right) at 400, 440, 480, 520, 560, and 600 nm.

weight 600, branched) under MT reaction conditions, similar to the preparation reported previously.[63] The FT-IR spectrum of the obtained dot sample is compared in Figure 6 with those of the above discussed CDots from the PEI−CA precursor mixture. On comparison, similar absorption features in the carbonyl region (1770−1650 cm^{-1}) may also be attributed to carboxylic acid−amino zwitterionic pairs in the dots, as the precursor carbon nanoparticles were oxidized in the nitric acid treatment, with the surface-bound carboxylic acid moieties capable of forming zwitterionic pairs with amino groups in the mixture used in the MT processing. The weaker and broader N−H and C−H absorptions of the PEI-CDots than those of PEI may also be attributed to some of the PEI species being partially scarified in the thermal processing and the generally more diverse local environments in the surface layer of the dots for the vibration modes under consideration.[64]

The visible absorption spectrum of the PEI-CDots agrees well with that of the EDA-CDots, thus also tracking closely that of the carbon nanoparticles (Figure 3) and exhibiting no extra absorptions as those found in some of the other CDots (Figure 3). The spectroscopic results suggest that the PEI-CDots may serve as an alternative to the EDA-CDots in those uses that exploit their absorption and fluorescence emission properties because the deliberate chemical functionalization synthesis for CDots similar to the EDA-CDots generally involves more steps and therefore is more time-consuming and less efficient than the hybrid approach used for the PEI-CDots.

For all of these CDots, there were characteristic excitation wavelength dependencies in the observed fluorescence spectra and quantum yields, where the "characteristic" refers to the dependencies following a generally rather similar pattern in the visible spectral region (Figures 7 and 8).[49,65] Again, the emphasis on the optical properties of CDots in the visible spectrum is important because it is in this spectral region that the optical absorptions of the carbon nanoparticles and CDots are essentially the same when the special surface passivation effects for the extra absorptions are absent. As shown in Figures 7 and 8, for example, the observed fluorescence spectra progressively move to the red with longer excitation wavelengths, which are accompanied by progressively decreasing fluorescence quantum yields. Also, characteristic and interesting is the fact that the excitation wavelength dependence of fluorescence quantum yields tracks closely the absorption spectral profile, except for those CDots with extra absorptions in the blue spectral region (Figures 7 and 8). For example, fluorescence spectra of the PEI-CDots at a series of different excitation wavelengths (Figure 7) are similar to those of the EDA-CDots and so are their corresponding fluorescence quantum yields (Figure 7). The comparisons between the PEI/CA-CDots$_{HT}$ and PEI/CA-CDots$_{MT}$ are also similar, except for excitations in the 400−460 nm region where there are noticeably different dependencies in fluorescence quantum yields between the two dot samples (Figure 8). The quantum yields for the PEI/CA-CDots$_{HT}$ are significantly higher, which are correlated with the more pronounced extra absorptions in the same blue spectral region. In fact, the PEI/CA-CDots$_{HT}$ is similar to the EPA-CDots with respect to the excitation wavelength dependence of fluorescence quantum yields (Figure 8), and for the latter, the extra absorptions in the blue spectral region are particularly pronounced (Figure 3). It seems that the special surface passivation effects proposed as being responsible for the extra absorptions are sensitive to the detailed configuration in the soft corona-like shell of the dot structure (Figure 1) and by extension dependent on the dot

DOI: 10.1021/acs.jpcc.8b06998
J. Phys. Chem. C 2018, 122, 21667−21676

synthesis, including different processing conditions. The comparison between PEI/CA-CDots$_{HT}$ and PEI/CA-CDots$_{MT}$ represents a particularly vivid demonstration in this regard because the only difference in the preparation of the two dot samples is with their processing conditions.

More generally, the results and comparisons presented above suggest that the CDots prepared in the three different syntheses and under different reaction conditions are at least qualitatively consistent in optical properties over the visible spectral region, despite some expected variations in structural details among these CDots. This is particularly noteworthy with respect to the comparison between CDots prepared by the first two approaches and their generally consistent spectroscopic results, which may be attributed to the dominance by the surface-functionalized/surface-passivated carbon nanoparticles in both absorptions and fluorescence emissions. On the carbonization of organic precursors in the second approach, insufficient carbonization because of the use of overly mild processing conditions may be responsible for the seemingly wide variations in products whose optical absorptions are confined mostly in the UV region and the associated diverse interpretations causing ongoing confusions and debates. When pushed further with more robust processing conditions in the carbonization, as those used in this study for the PEI/CA-CDots$_{HT}$ and PEI/CA-CDots$_{MT}$, there must be convergence toward the formation of carbon nanoparticles at the expense of the initially formed various products referred to above. The CDots thus produced, again the PEI/CA-CDots$_{HT}$ and PEI/CA-CDots$_{MT}$ as specific examples, are no different spectroscopically from the reference CDots by the deliberate chemical functionalization in the first approach. Structurally, however, much remains to be investigated on the "core carbon nanoparticles" in CDots from the carbonization synthesis, as it might be imagined that they would be more porous than the pre-existing carbon nanoparticles sourced from pure carbon soot, with likely more nitrogen content because of the use of nitrogen-containing precursors in the carbonization. The insensitivity of observed optical absorptions and fluorescence emissions in the visible spectrum, as noticed in previous studies as well,[66] does not support any substantial effects because of the nitrogen doping of the carbon nanoparticles in CDots. In fact, it seems more obvious that the general definition on CDots as surface-passivated small carbon nanoparticles is relatively flexible or stable in terms of tolerating some variations in structural details. This may be viewed from a different angle, such that CDots represent a rather stable nanomaterial configuration for the generally consistent optical properties over the visible spectral region, where the photon absorptions are dictated by the core carbon nanoparticles, including those in the PEI/CA-CDots$_{HT}$ and PEI/CA-CDots$_{MT}$ prepared by the carbonization method under sufficiently robust processing conditions.

In addition to the optical properties in the visible spectrum discussed above, CDots are known for their characteristic photoinduced redox properties as both excellent electron acceptors and donors.[41,67−69] Most investigations have been on CDots prepared by the deliberate chemical functionalization method, demonstrating the highly efficient fluorescence quenching by electron-rich and -deficient molecules such as DEA and DNT, respectively.[65,67,68] The same redox quenchers were used in this study for the evaluation of the CDots from different syntheses and under different processing conditions. The results summarized in Table 2 suggest that all of these

Table 2. Stern−Volmer Parameters for Fluorescence Quenching of the CDots by Electron Donor and Acceptor

	DEA[a]		DNT[a]	
dot sample	K_{SV} (M^{-1})	k_q (10^9 M^{-1} s^{-1})	K_{SV} (M^{-1})	k_q (10^9 M^{-1} s^{-1})
EDA-CDots[b,c]	18.5	2.6	89[d]	12.5
EPA-CDots	11	1.3	176[d,e]	21
PEG$_{1500N}$-CDots[f]	19	4.8	32	8
PEI/CA-CDots$_{HT}$	12.3	0.9	75[d]	5.5
PEI/CA-CDots$_{MT}$	11	0.88	65[d]	5.2
PEI-CDots	26	3.5	52[d]	7

[a]With excitation at 440 nm unless otherwise noted. [b]From refs 65 and 68. [c]With excitation at 425 nm excitation. [d]From fitting the linear portion of the plot for low quencher concentrations. [e]If based on fluorescence lifetime quenching and a fit of the plot for low quencher concentrations only, K_{SV} = 106, and the corresponding k_q = 12.6 × 10^9 M^{-1} s^{-1}. [f]From ref 67, with excitation at 400 nm for DEA and 407 nm for DNT.

CDots are generally potent electron acceptors and donors in the fluorescence quenching, although relatively they are better donors than acceptors. For the comparison between the PEI/CA-CDots$_{HT}$ and PEI/CA-CDots$_{MT}$ as a representative example, Stern−Volmer plots for the fluorescence quenching by DEA in ethanol solution are both linear (Figure 9), yielding

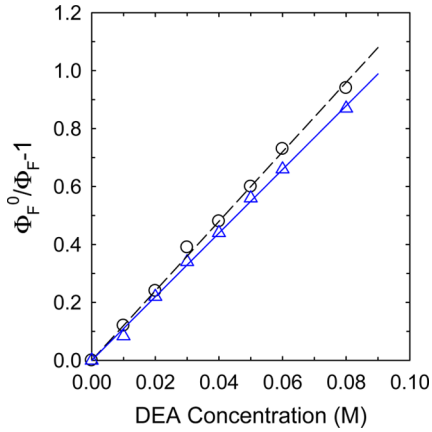

Figure 9. Stern−Volmer plots for the quenching of fluorescence intensities (quantum yields) (440 nm excitation) of the PEI/CA-CDots$_{HT}$ (○, best fit - - -) and PEI/CA-CDots$_{MT}$ (Δ, best fit) by DEA in ethanol.

quenching constants (K_{SV}) of 12.3 and 11 M^{-1}, respectively. With their average fluorescence lifetimes $\langle\tau_F\rangle$ (Table 1, approximated as τ_F° in the Stern−Volmer equation) of 14 and 12.5 ns, the corresponding quenching rate constants (k_q = K_{SV}/τ_F°) of both around 0.9 × 10^9 M^{-1} s^{-1} are at the limit of diffusion control. On the other hand, for both dot samples, the fluorescence quenching by DNT is extremely efficient, with Stern−Volmer plots not only steeper but also curved upward because of significant static-quenching contributions at still relatively low DNT concentrations (Figure 10). By fitting the linear portion only (corresponding to DNT concentrations of 0.04 M and lower), the K_{SV} values are 75 M^{-1} for the PEI/CA-CDots$_{HT}$ and 65 M^{-1} for the PEI/CA-CDots$_{MT}$, and the corresponding k_q values of 5.5 × 10^9 and 5.2 × 10^9 M^{-1} s^{-1}, respectively, are both at or beyond the upper end of diffusion control.

DOI: 10.1021/acs.jpcc.8b06998
J. Phys. Chem. C 2018, 122, 21667−21676

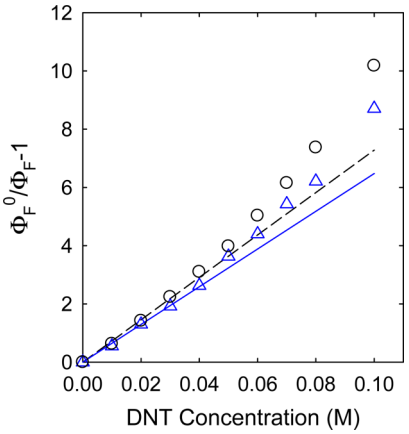

Figure 10. Stern–Volmer plots for the quenching of fluorescence intensities (quantum yields) (440 nm excitation) of the PEI/CA-CDots$_{HT}$ (○, best fit for quencher concentrations of 0.03 M and lower - - -) and PEI/CA-CDots$_{MT}$ (Δ, best fit for quencher concentrations of 0.04 M and lower) by DNT in ethanol.

The fluorescence quenching results (Table 2) suggest that CDots regardless of their syntheses (considering especially the major difference between the use of pre-existing carbon nanoparticles in the first and third approaches and the formation of presumably similar nanoparticles via carbonization processing in the second approach) and processing conditions are generally potent electron acceptors and at the same time extraordinary electron donors. Specifically on DNT as a representative electron-deficient quencher for all of these CDots, static quenching contributions are significant even at low or very low DNT concentrations, and Stern–Volmer plots for the linear portion including only the low DNT concentrations yield abnormally large K_{SV} values (Table 2), from which the calculated quenching rate constants (k_q) are beyond diffusion control. Mechanistically, the seemingly larger than realistic k_q values are consistent with the observed substantial static quenching contributions, as both reflect the extraordinary photoinduced electron-donating abilities of CDots, and both can be rationalized as being due to an enlarged quenching radius beyond the boundary of the dot surface.[68] The highly potent electron donor characteristics of CDots are also consistent with or responsible for their already demonstrated effective photocatalytic functions in some of the most challenging photoreduction reactions, such as the photocatalytic reduction of CO_2 into small organic molecules.[11,33] The results presented and discussed here suggest that CDots from different synthetic schemes can all be used as potentially efficient photocatalysts for related applications.

CONCLUSIONS

The three synthesis approaches for CDots compared in this study were based on the use of pre-existing small carbon nanoparticles sourced from pure carbon soot versus the formation of similar nanoparticles (at least for their optical absorptions in the visible spectrum) via carbonization processing. The results show that the CDots from the latter under sufficiently robust processing conditions are generally no different from those from the former in terms of the observed optical properties and associated photoinduced redox characteristics in the visible spectral region, which is the region more meaningful to most of the widely pursued technological applications of CDots. The results also suggest a high stability or general applicability of the definition on CDots as surface-passivated small carbon nanoparticles. Further investigations are needed for a clear mechanistic understanding of CDots, also addressing the ongoing issues in the UV spectral region for some of the samples prepared via carbonization processing under overly mild processing conditions. In any case, the focus should be on the small carbon nanoparticles, which are at the core of the CDots platform both conceptually and structurally and also as defined recently,[70] represent another zero-dimensional carbon allotrope (in addition to fullerenes), with major fundamental and technological implications.

AUTHOR INFORMATION

Corresponding Authors

*E-mail: sungrp@clemson.edu (P.W.).
*E-mail: lyang@nccu.edu (L.Y.).
*E-mail: syaping@clemson.edu (Y.-P.S.).

ORCID

Ya-Ping Sun: 0000-0001-8593-5769

Notes

The authors declare no competing financial interest.

ACKNOWLEDGMENTS

Financial support from NSF (DMR-1701399 and DMR-1701424), NIH (R15GM114752), Air Force Research Laboratory, and South Carolina Space Grant Consortium is gratefully acknowledged.

REFERENCES

(1) Sun, Y.-P.; Zhou, B.; Lin, Y.; Wang, W.; Fernando, K. A. S.; Pathak, P.; Meziani, M. J.; Harruff, B. A.; Wang, X.; Wang, H.; et al. Quantum-Sized Carbon Dots for Bright and Colorful Photoluminescence. *J. Am. Chem. Soc.* **2006**, *128*, 7756–7757.
(2) Sun, Y.-P. Fluorescent Carbon Nanoparticles. U.S. Patent 7,829,772 B2, 2010.
(3) Cao, L.; Meziani, M. J.; Sahu, S.; Sun, Y.-P. Photoluminescence Properties of Graphene versus Other Carbon Nanomaterials. *Acc. Chem. Res.* **2013**, *46*, 171–180.
(4) LeCroy, G. E.; Yang, S.-T.; Yang, F.; Liu, Y.; Fernando, K. A. S.; Bunker, C. E.; Hu, Y.; Luo, P. G.; Sun, Y.-P. Functionalized Carbon Nanoparticles: Syntheses and Applications in Optical Bioimaging and Energy Conversion. *Coord. Chem. Rev.* **2016**, *320–321*, 66–81.
(5) Yang, S.-T.; Cao, L.; Luo, P. G.; Lu, F.; Wang, X.; Wang, H.; Meziani, M. J.; Liu, Y.; Qi, G.; Sun, Y.-P. Carbon Dots for Optical Imaging in Vivo. *J. Am. Chem. Soc.* **2009**, *131*, 11308–11309.
(6) Kong, B.; Zhu, A.; Ding, C.; Zhao, X.; Li, B.; Tian, Y. Carbon Dot-Based Inorganic-Organic Nanosystem for Two-Photon Imaging and Biosensing of pH Variation in Living Cells and Tissues. *Adv. Mater.* **2012**, *24*, 5844–5848.
(7) Song, Y.; Zhu, S.; Yang, B. Bioimaging Based on Fluorescent Carbon dots. *RSC Adv.* **2014**, *4*, 27184–27200.
(8) Ge, J.; Jia, Q.; Liu, W.; Guo, L.; Liu, Q.; Lan, M.; Zhang, H.; Meng, X.; Wang, P. Red-Emissive Carbon Dots for Fluorescent, Photoacoustic, and Thermal Theranostics in Living Mice. *Adv. Mater.* **2015**, *27*, 4169–4177.
(9) Liu, J.-H.; Cao, L.; LeCroy, G. E.; Wang, P.; Meziani, M. J.; Dong, Y.; Liu, Y.; Luo, P. G.; Sun, Y.-P. Carbon Quantum Dots for Fluorescence Labeling of Cells. *ACS Appl. Mater. Interfaces* **2015**, *7*, 19439–19445.
(10) Loo, A. H.; Sofer, Z.; Bouša, D.; Ulbrich, P.; Bonanni, A.; Pumera, M. Carboxylic Carbon Quantum Dots as A Fluorescent Sensing Platform for DNA Detection. *ACS Appl. Mater. Interfaces* **2016**, *8*, 1951–1957.
(11) Cao, L.; Sahu, S.; Anilkumar, P.; Bunker, C. E.; Xu, J.; Fernando, K. A. S.; Wang, P.; Guliants, E. A.; Tackett, K. N.; Sun, Y.-

DOI: 10.1021/acs.jpcc.8b06998
J. Phys. Chem. C 2018, 122, 21667–21676

P. Carbon Nanoparticles as Visible-Light Photocatalysts for Efficient CO2Conversion and Beyond. *J. Am. Chem. Soc.* **2011**, *133*, 4754−4757.
(12) Wang, F.; Chen, Y.-h.; Liu, C.-y.; Ma, D.-g. White Light-Emitting Devices Based on Carbon Dots Electroluminescence. *Chem. Commun.* **2011**, *47*, 3502−3504.
(13) Mirtchev, P.; Henderson, E. J.; Soheilnia, N.; Yip, C. M.; Ozin, G. A. Solution phase synthesis of carbon quantum dots as sensitizers for nanocrystalline TiO2solar cells. *J. Mater. Chem.* **2012**, *22*, 1265−1269.
(14) Narayanan, R.; Deepa, M.; Srivastava, A. K. Förster resonance energy transfer and carbon dots enhance light harvesting in a solid-state quantum dot solar cell. *J. Mater. Chem. A* **2013**, *1*, 3907−3918.
(15) Briscoe, J.; Marinovic, A.; Sevilla, M.; Dunn, S.; Titirici, M. Biomass-Derived Carbon Quantum Dot Sensitizers for Solid-State Nanostructured Solar Cells. *Angew. Chem., Int. Ed.* **2015**, *54*, 4463−4468.
(16) Du, J.; Zhao, Y.; Chen, J.; Zhang, P.; Gao, L.; Wang, M.; Cao, C.; Wen, W.; Zhu, C. Difunctional Cu-Doped Carbon Dots: Catalytic Activity and Fluorescence Indication for The Reduction Reaction of P-Nitrophenol. *RSC Adv.* **2017**, *7*, 33929−33936.
(17) Meziani, M. J.; Dong, X.; Zhu, L.; Jones, L. P.; LeCroy, G. E.; Yang, F.; Wang, S.; Wang, P.; Zhao, Y.; Yang, L.; et al. Visible-Light-Activated Bactericidal Functions of Carbon Quantum Dots. *ACS Appl. Mater. Interfaces* **2016**, *8*, 10761−10766.
(18) Bing, W.; Sun, H.; Yan, Z.; Ren, J.; Qu, X. Programmed Bacteria Death Induced by Carbon Dots with Different Surface Charge. *Small* **2016**, *12*, 4713−4718.
(19) Yang, J.; Zhang, X.; Ma, Y.-H.; Gao, G.; Chen, X.; Jia, H.-R.; Li, Y.-H.; Chen, Z.; Wu, F.-G. Carbon Dot-Based Platform for Simultaneous Bacterial Distinguishment and Antibacterial Applications. *ACS Appl. Mater. Interfaces* **2016**, *8*, 32170−32181.
(20) Dong, X.; Moyer, M.; Yang, F.; Sun, Y.-P.; Yang, L. Carbon Dots' Antiviral Functions Against Noroviruses. *Sci. Rep.* **2017**, *7*, 519.
(21) Jhonsi, M. A.; Ananth, D. A.; Nambirajan, G.; Sivasudha, T.; Yamini, R.; Bera, S.; Kathiravan, A. Antimicrobial Activity, Cytotoxicity and DNA Binding Studies of Carbon Dots. *Spectrochim. Acta, Part A* **2018**, *196*, 295−302.
(22) Wang, R.; Li, G.; Dong, Y.; Chi, Y.; Chen, G. Carbon Quantum Dot-Functionalized Aerogels for NO2 Gas Sensing. *Anal. Chem.* **2013**, *85*, 8065−8069.
(23) Han, X.; Zhong, S.; Pan, W.; Shen, W. A Simple Strategy for Synthesizing Highly Luminescent Carbon Nanodots and Application as Effective Down-Shifting Layers. *Nanotechnology* **2015**, *26*, 065402.
(24) Xu, Z.-Q.; Lan, J.-Y.; Jin, J.-C.; Dong, P.; Jiang, F.-L.; Liu, Y. Highly Photoluminescent Nitrogen-Doped Carbon Nanodots and Their Protective Effects against Oxidative Stress on Cells. *ACS Appl. Mater. Interfaces* **2015**, *7*, 28346−28352.
(25) Bhattacharyya, S.; Ehrat, F.; Urban, P.; Teves, R.; Wyrwich, R.; Döblinger, M.; Feldmann, J.; Urban, A. S.; Stolarczyk, J. K. Effect of Nitrogen Atom Positioning on the Trade-Off Between Emissive and Photocatalytic Properties of Carbon Dots. *Nat. Commun.* **2017**, *8*, 1401.
(26) Vázquez-González, M.; Liao, W.-C.; Cazelles, R.; Wang, S.; Yu, X.; Gutkin, V.; Willner, I. Mimicking Horseradish Peroxidase Functions Using Cu2+-Modified Carbon Nitride Nanoparticles or Cu2+-Modified Carbon Dots as Heterogeneous Catalysts. *ACS Nano* **2017**, *11*, 3247−3253.
(27) Sun, X.; Lei, Y. Fluorescent Carbon Dots and Their Sensing Applications. *Trends Anal. Chem.* **2017**, *89*, 163−180.
(28) Wang, R.; Lu, K.-Q.; Tang, Z.-R.; Xu, Y.-J. Recent Progress in Carbon Quantum Dots: Synthesis, Properties and Applications in Photocatalysis. *J. Mater. Chem. A* **2017**, *5*, 3717−3734.
(29) Wang, J.; Choi, H. S.; Wang, Y.-X. J. Exponential Growth of Publications on Carbon Nanodots by Chinese Authors. *J. Thorac. Dis.* **2015**, *7*, E201−E205.
(30) Roy, P.; Chen, P.-C.; Periasamy, A. P.; Chen, Y.-N.; Chang, H.-T. Photoluminescent Carbon Nanodots: Synthesis, Physicochemical Properties and Analytical Applications. *Mater. Today* **2015**, *18*, 447−458.
(31) Lim, S. Y.; Shen, W.; Gao, Z. Carbon Quantum Dots and Their Applications. *Chem. Soc. Rev.* **2015**, *44*, 362−381.
(32) Georgakilas, V.; Perman, J. A.; Tucek, J.; Zboril, R. Broad Family of Carbon Nanoallotropes: Classification, Chemistry, and Applications of Fullerenes, Carbon Dots, Nanotubes, Graphene, Nanodiamonds, and Combined Superstructures. *Chem. Rev.* **2015**, *115*, 4744−4822.
(33) Fernando, K. A. S.; Sahu, S.; Liu, Y.; Lewis, W. K.; Guliants, E. A.; Jafariyan, A.; Wang, P.; Bunker, C. E.; Sun, Y.-P. Carbon Quantum Dots and Applications in Photocatalytic Energy Conversion. *ACS Appl. Mater. Interfaces* **2015**, *7*, 8363−8376.
(34) Yuan, F.; Li, S.; Fan, Z.; Meng, X.; Fan, L.; Yang, S. Shining Carbon Dots: Synthesis and Biomedical and Optoelectronic Applications. *Nano Today* **2016**, *11*, 565−586.
(35) Wang, J.; Qiu, J. A Review of Carbon Dots in Biological Applications. *J. Mater. Sci.* **2016**, *51*, 4728−4738.
(36) Zuo, P.; Lu, X.; Sun, Z.; Guo, Y.; He, H. A Review on Syntheses, Properties, Characterization and Bioanalytical Applications of Fluorescent Carbon Dots. *Microchim. Acta* **2016**, *183*, 519−542.
(37) Zhou, J.; Zhou, H.; Tang, J.; Deng, S.; Yan, F.; Li, W.; Qu, M. Carbon Dots Doped with Heteroatoms for Fluorescent Bioimaging: A Review. *Microchim. Acta* **2017**, *184*, 343−368.
(38) Peng, Z.; Han, X.; Li, S.; Al-Youbi, A. O.; Bashammakh, A. S.; El-Shahawi, M. S.; Leblanc, R. M. Carbon Dots: Biomacromolecule Interaction, Bioimaging and Nanomedicine. *Coord. Chem. Rev.* **2017**, *343*, 256−277.
(39) Essner, J. B.; Baker, G. A. The Emerging Roles of Carbon Dots in Solar Photovoltaics: A Critical Review. *Environ. Sci.: Nano* **2017**, *4*, 1216−1263.
(40) Namdari, P.; Negahdari, B.; Eatemadi, A. Synthesis, Properties and Biomedical Applications of Carbon-Based Quantum Dots: An Updated Review. *Biomed. Pharmacother.* **2017**, *87*, 209−222.
(41) Hutton, G. A. M.; Martindale, B. C. M.; Reisner, E. Carbon Dots as Photosensitisers for Solar-Driven Catalysis. *Chem. Soc. Rev.* **2017**, *46*, 6111−6123.
(42) Wang, X.; Cao, L.; Yang, S.-T.; Lu, F.; Meziani, M. J.; Tian, L.; Sun, K. W.; Bloodgood, M. A.; Sun, Y.-P. Bandgap-Like Strong Fluorescence in Functionalized Carbon Nanoparticles. *Angew. Chem., Int. Ed.* **2010**, *122*, 5438−5442.
(43) LeCroy, G. E.; Sonkar, S. K.; Yang, F.; Veca, L. M.; Wang, P.; Tackett, K. N.; Yu, J.-J.; Vasile, E.; Qian, H.; Liu, Y.; et al. Toward Structurally Defined Carbon Dots as Ultracompact Fluorescent Probes. *ACS Nano* **2014**, *8*, 4522−4529.
(44) Anilkumar, P.; Wang, X.; Cao, L.; Sahu, S.; Liu, J.-H.; Wang, P.; Korch, K.; Tackett, K. N., II; Parenzan, A.; Sun, Y.-P. Toward quantitatively fluorescent carbon-based quantum dots. *Nanoscale* **2011**, *3*, 2023−2027.
(45) Dong, Y.; Wang, R.; Li, H.; Shao, J.; Chi, Y.; Lin, X.; Chen, G. Polyamine-Functionalized Carbon Quantum Dots for Chemical Sensing. *Carbon* **2012**, *50*, 2810−2815.
(46) Dong, Y.; Wang, R.; Li, G.; Chen, C.; Chi, Y.; Chen, G. Polyamine-Functionalized Carbon Quantum Dots as Fluorescent Probes for Selective and Sensitive Detection of Copper Ions. *Anal. Chem.* **2012**, *84*, 6220−6224.
(47) Liu, J.; Liu, X.; Luo, H.; Gao, Y. One-Step Preparation of Nitrogen-Doped and Surface-Passivated Carbon Quantum Dots with High Quantum Yield and Excellent Optical Properties. *RSC Adv.* **2014**, *4*, 7648−7654.
(48) Wang, C.; Xu, Z.; Zhang, C. Polyethyleneimine-Functionalized Fluorescent Carbon Dots: Water Stability, pH Sensing, and Cellular Imaging. *ChemNanoMat* **2015**, *1*, 122−127.
(49) Hou, X.; Hu, Y.; Wang, P.; Yang, L.; Al Awak, M. M.; Tang, Y.; Twara, F. K.; Qian, H.; Sun, Y.-P. Modified Facile Synthesis for Quantitatively Fluorescent Carbon Dots. *Carbon* **2017**, *122*, 389−394.

DOI: 10.1021/acs.jpcc.8b06998
J. Phys. Chem. C 2018, 122, 21667−21676

(50) Krysmann, M. J.; Kelarakis, A.; Dallas, P.; Giannelis, E. P. Formation Mechanism of Carbogenic Nanoparticles with Dual Photoluminescence Emission. *J. Am. Chem. Soc.* **2012**, *134*, 747−750.
(51) Zhu, S.; Song, Y.; Zhao, X.; Shao, J.; Zhang, J.; Yang, B. The Photoluminescence Mechanism in Carbon Dots (Graphene Quantum Dots, Carbon Nanodots, and Polymer Dots): Current State and Future Perspective. *Nano Res.* **2015**, *8*, 355−381.
(52) Song, Y.; Zhu, S.; Zhang, S.; Fu, Y.; Wang, L.; Zhao, X.; Yang, B. Investigation from Chemical Structure to Photoluminescent Mechanism: A Type of Carbon Dots from the Pyrolysis of Citric Acid and An Amine. *J. Mater. Chem. C* **2015**, *3*, 5976−5984.
(53) Fu, M.; Ehrat, F.; Wang, Y.; Milowska, K. Z.; Reckmeier, C.; Rogach, A. L.; Stolarczyk, J. K.; Urban, A. S.; Feldmann, J. Carbon Dots: A Unique Fluorescent Cocktail of Polycyclic Aromatic Hydrocarbons. *Nano Lett.* **2015**, *15*, 6030−6035.
(54) Shi, L.; Yang, J. H.; Zeng, H. B.; Chen, Y. M.; Yang, S. C.; Wu, C.; Zeng, H.; Yoshihito, O.; Zhang, Q. Carbon Dots with High Fluorescence Quantum Yield: the Fluorescence Originates from Organic Fluorophores. *Nanoscale* **2016**, *8*, 14374−14378.
(55) Ehrat, F.; Bhattacharyya, S.; Schneider, J.; Löf, A.; Wyrwich, R.; Rogach, A. L.; Stolarczyk, J. K.; Urban, A. S.; Feldmann, J. Tracking the Source of Carbon Dot Photoluminescence: Aromatic Domains versus Molecular Fluorophores. *Nano Lett.* **2017**, *17*, 7710−7716.
(56) Dong, Y.; Pang, H.; Yang, H. B.; Guo, C.; Shao, J.; Chi, Y.; Li, C. M.; Yu, T. Carbon-Based Dots Co-doped with Nitrogen and Sulfur for High Quantum Yield and Excitation-Independent Emission. *Angew. Chem.* **2013**, *125*, 7954−7958.
(57) Guo, Y.; Wang, Z.; Shao, H.; Jiang, X. Hydrothermal Synthesis of Highly Fluorescent Carbon Nanoparticles from Sodium Citrate and Their Use for the Detection of Mercury Ions. *Carbon* **2013**, *52*, 583−589.
(58) Yang, Z.; Xu, M.; Liu, Y.; He, F.; Gao, F.; Su, Y.; Wei, H.; Zhang, Y. Nitrogen-Doped, Carbon-Rich, Highly Photoluminescent Carbon Dots From Ammonium Citrate. *Nanoscale* **2014**, *6*, 1890−1895.
(59) Xu, Q.; Pu, P.; Zhao, J.; Dong, C.; Gao, C.; Chen, Y.; Chen, J.; Liu, Y.; Zhou, H. Preparation of Highly Photoluminescent Sulfur-Doped Carbon Dots for Fe(iii) Detection. *J. Mater. Chem. A* **2015**, *3*, 542−546.
(60) Yang, F.; LeCroy, G. E.; Wang, P.; Liang, W.; Chen, J.; Fernando, K. A. S.; Bunker, C. E.; Qian, H.; Sun, Y.-P. Functionalization of Carbon Nanoparticles and Defunctionalization-Toward Structural and Mechanistic Elucidation of Carbon Quantum Dots. *J. Phys. Chem. C* **2016**, *120*, 25604−25611.
(61) Yang, S.-T.; Wang, X.; Wang, H.; Lu, F.; Luo, P. G.; Cao, L.; Meziani, M. J.; Liu, J.-H.; Liu, Y.; Chen, M.; et al. Carbon Dots as Nontoxic and High-Performance Fluorescence Imaging Agents. *J. Phys. Chem. C* **2009**, *113*, 18110−18114.
(62) Xu, J.; Sahu, S.; Cao, L.; Anilkumar, P.; Tackett, K. N.; Qian, H.; Bunker, C. E.; Guliants, E. A.; Parenzan, A.; Sun, Y.-P. Carbon Nanoparticles as Chromophores for Photon Harvesting and Photoconversion. *ChemPhysChem* **2011**, *12*, 3604−3608.
(63) Hu, Y.; Al Awak, M. M.; Yang, F.; Yan, S.; Xiong, Q.; Wang, P.; Tang, Y.; Yang, L.; LeCroy, G. E.; Hou, X.; et al. Photoexcited State Properties of Carbon Dots from Thermally Induced Functionalization of Carbon Nanoparticles. *J. Mater. Chem. C* **2016**, *4*, 10554−10561.
(64) Liu, Y.; Wang, P.; Shiral Fernando, K. A.; LeCroy, G. E.; Maimaiti, H.; Harruff-Miller, B. A.; Lewis, W. K.; Bunker, C. E.; Hou, Z.-L.; Sun, Y.-P. Enhanced Fluorescence Properties of Carbon Dots in Polymer Films. *J. Mater. Chem. C* **2016**, *4*, 6967−6974.
(65) LeCroy, G. E.; Messina, F.; Sciortino, A.; Bunker, C. E.; Wang, P.; Fernando, K. A. S.; Sun, Y.-P. Characteristic Excitation Wavelength Dependence of Fluorescence Emissions in Carbon Quantum Dots. *J. Phys. Chem. C* **2017**, *121*, 28180−28186.
(66) Wang, Y.; Anilkumar, P.; Cao, L.; Liu, J.-H.; Luo, P. G.; Tackett, K. N.; Sahu, S.; Wang, P.; Wang, X.; Sun, Y.-P. Carbon dots of different composition and surface functionalization: cytotoxicity issues relevant to fluorescence cell imaging. *Exp. Biol. Med.* **2011**, *236*, 1231−1238.
(67) Wang, X.; Cao, L.; Lu, F.; Meziani, M. J.; Li, H.; Qi, G.; Zhou, B.; Harruff, B. A.; Kermarrec, F.; Sun, Y.-P. Photoinduced Electron Transfers with Carbon Dots. *Chem. Commun.* **2009**, 3774−3776.
(68) LeCroy, G. E.; Fernando, K. A. S.; Bunker, C. E.; Wang, P.; Tomlinson, N.; Sun, Y.-P. Steady-state and time-resolved fluorescence studies on interactions of carbon quantum dots with nitrotoluenes. *Inorg. Chim. Acta* **2017**, *468*, 300−307.
(69) Zu, F.; Yan, F.; Bai, Z.; Xu, J.; Wang, Y.; Huang, Y.; Zhou, X. The Quenching of the Fluorescence of Carbon Dots: A Review on Mechanisms and Applications. *Microchim. Acta* **2017**, *184*, 1899−1914.
(70) Yang, F.; Ren, X.; LeCroy, G. E.; Song, J.; Wang, P.; Beckerle, L.; Bunker, C. E.; Xiong, Q.; Sun, Y.-P. Zero-Dimensional Carbon Allotropes-Carbon Nanoparticles Versus Fullerenes in Functionalization by Electronic Polymers for Different Optical and Redox Properties. *ACS Omega* **2018**, *3*, 5685−5691.

DOI: 10.1021/acs.jpcc.8b06998
J. Phys. Chem. C 2018, 122, 21667−21676